

# Effect of thermal treatment on the mechanical and toughness properties of extruded SiC<sub>w</sub>/aluminium 6061 metal matrix composite

D. F. HASSON

*Department of Mechanical Engineering, US Naval Academy, Annapolis, Maryland 21402, USA*

S. M. HOOVER

*Research Department, US Naval Surface Weapons Center, Silver Spring, Maryland 20910, USA*

C. R. CROWE

*Materials Science and Technology, US Naval Research Laboratory, Washington, DC 20375, USA*

Mechanical, instrumented Charpy V-notch (CVN) energy and plane strain fracture toughness properties of SiC whisker reinforced-6061 aluminium metal matrix composite material from an extruded tube have been determined. The effect of thermal treatment and orientation have been studied. The mechanical strength properties are higher than wrought Al 6061 in the T6 condition. CVN energy values, however, were reduced by an order of magnitude.  $K_{Ic}$  fracture toughness of the as-received, T6 and degassed + T6 thermal treatments were 50% of the wrought Al 6061 alloy. The effect of orientation showed that the orientation with the least amount of SiC whisker in the crack plane (i.e. greatest mean free path between reinforcements) yields the highest toughness value.

## 1. Introduction

Discontinuous silicon carbide/aluminium alloy (SiC/Al) metal matrix composites (MMCs) have exhibited improved physical and mechanical properties as compared to the wrought properties of the matrix alloy. These improved properties include high specific modulus, high creep strength, high fatigue resistance, low thermal expansion and good thermal stability [1-9]. The SiC/Al composite can also be worked using standard metallurgical processing and hence is inexpensive to produce compared to other MMC systems. The tensile ductility and fracture properties of the composite reported to date, however, are less than wrought alloy properties [1, 10-15]. The tensile ductility has been

improved by control of process parameters, but relatively little improvement in fracture toughness has been achieved. The possibility of fracture toughness improvement by thermal treatment is another approach and this is the object of the present study. Orientation effects on fracture toughness are also studied.

## 2. Experimental procedure

### 2.1. Materials

The materials were 20 vol % SiC whisker/reinforced aluminium 6061 composite (20 vol % SiC<sub>w</sub>/Al 6061) from a 31.8 mm wall thickness, 320 mm diameter extruded cylinder. The SiC used to form the composite was a mixture of fine whiskers and particles with whisker content

TABLE I Chemical analyses (wt %) for wrought Al 6061 and composite SiC<sub>w</sub>/Al 6061 from extruded tube

Element	Wrought Al 6061	Composite SiC <sub>w</sub> /Al 6061
Mg	0.82	0.66
Si	0.68	—
Cr	0.16	0.18
Cu	0.18	0.39
Fe	0.44	0.65
Mn	0.06	0.08
Ni	0.01	0.01
Zn	0.11	0.03
Ti	0.01	0.03
SiC	—	25.41
C	—	7.61
O	—	0.4530
H	—	0.0005
N	—	0.0871
Al	Remainder	Remainder

originally about 80%. The whiskers are  $\beta$ -SiC with diameters ranging from 0.2 to 1.0  $\mu\text{m}$  and original lengths up to 50  $\mu\text{m}$ . The whiskers were then blended with -325 mesh commercially available inert gas atomized Al 6061 powders. The composite was formed by cold compaction followed by hot pressing at temperatures above the solidus of the matrix to form as-pressed billet material. The billet was then extruded to form the tube.

TABLE II Description of thermal treatments to extruded tube materials

Condition	Thermal Treatment
As-received	None prior to testing
T6	Solution treated at 527° C for 1 h; cold water quenched; then precipitation hardened at 177° C for 8 h followed by air cool
Degassed	Heated to 500° C for 48 h in a 25 m torr vacuum. Specimen allowed to cool <i>in vacuo</i> .
Degassed + T6	Degas thermal treatment was used, then T6 thermal treatment was applied

The chemical analysis of the composite is given in Table I. The chemical analysis for wrought Al 6061 is given for comparison.

The microstructure of the material is given in Fig. 1. Fibres are generally aligned in the extrusion direction. The microstructure of the composite also shows that most of the whiskers were fragmented during the fabrication of the cylinder.

## 2.2. Thermal treatments

Specimens were cut from the cylinder and thermally treated as described in Table II to provide specimens of as-received, T6, degassed,

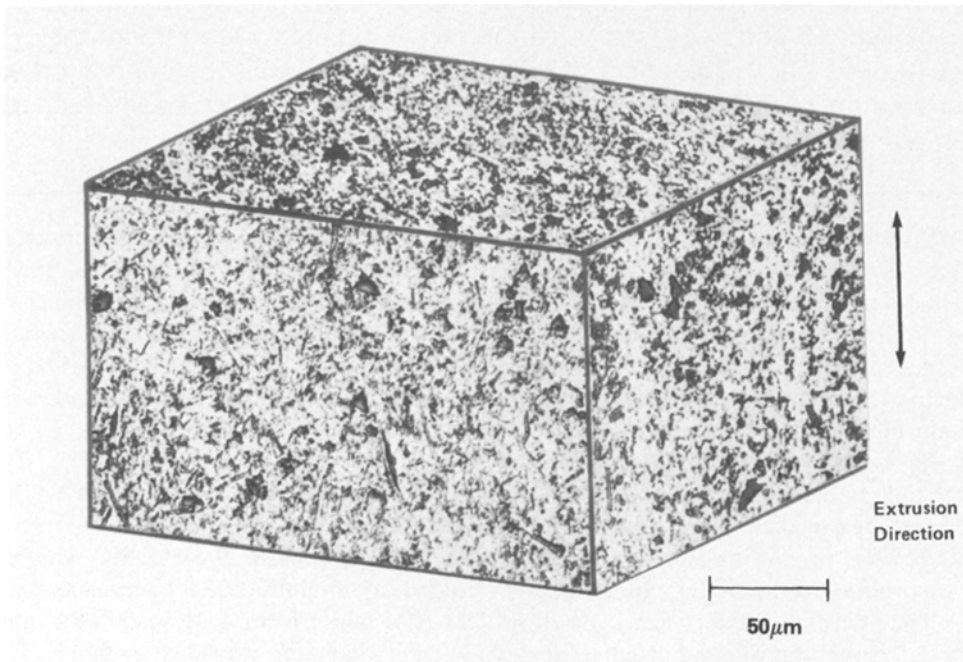


Figure 1 Microstructure of SiC<sub>w</sub>/Al 6061 extruded tube material.

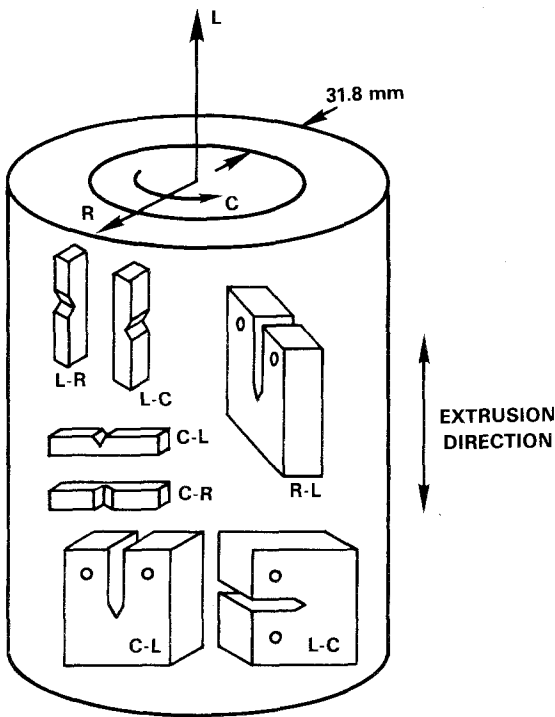


Figure 2 Orientation of specimens from extruded tube.

and degassed followed by a T6 thermal treatment.

### 2.3. Mechanical tests

Duplicate longitudinal orientation [16] 4.1 mm diameter tensile test specimens were fabricated and tested at room temperature to obtain modulus of elasticity, 0.2% offset yield stress, ultimate tensile stress and per cent elongation. Specimen orientations are shown in Fig. 2. Duplicate 12.8 mm as-received specimens were also tested to determine a possible test volume effect. Also Rockwell-B scale (HRB) measurements were made on the materials.

### 2.4. Toughness tests

Charpy V-notch (CVN) specimens were prepared from all thermal treatments in the L-C orientation. Triplicate specimens were tested at room temperature in an instrumented Charpy tester.

$K_{Ic}$  fracture toughness testing was performed on duplicate  $\frac{1}{2}$ T compact tensile specimens from all thermally treated materials in the L-C orientation. Degassed + T6 specimens were also tested in the R-L and C-L orientations. The testing and data analysis conformed to

ASTM E399 procedures [17] with the exception that the specimens were not fatigue precracked. Data from a separate study on the effect of notch acuity [18] was utilized to select a valid notch root radius. The study showed a valid  $K_{Ic}$  is obtained with a notch root radius of less than  $80 \mu\text{m}$ . The notch radius for the results reported herein was  $74 \mu\text{m}$ .

### 2.5. Fractography

Stereo pair scanning electron microscopy (SEM) along with energy dispersive X-ray analysis (EDAX) fractography was performed on representative fracture surfaces.

The dimple, height  $h$ , measurements were made from SEM stereo pairs using the relation

$$h = \frac{P}{2M} \left( \sin \frac{\phi}{2} \right)^{-1} \quad (1)$$

where  $P$  is the parallax,  $M$  is the magnification, and  $\phi$  is the tilt angle between the stereo pairs. Parallax is measured as the difference in distance between any two identifiable image points measured on one photograph and that same distance measured on the other photograph of the stereo pair.

## 3. Results and discussion

### 3.1. Mechanical properties

The mechanical properties for the various thermally treated longitudinal orientation specimens are given in Table III. Also included in Table III are reference values [19] for wrought Al 6061 in the T6 condition. Comparison of Al 6061-T6 and SiC<sub>w</sub>/Al 6061-T6 properties shows significant increases in modulus, yield stress and ultimate stress due to the addition of the SiC whiskers. Ductility, however, is less in the SiC<sub>w</sub>/Al 6061-T6 materials.

The extruded tube (as-received material) was supposed to be delivered in a T6 condition. The slightly lower values of yield stress and Rockwell-B hardness (HRB) can be attributed to overageing caused by lower cooling rates in the extruded tube during quenching following ageing. Also in the as-received material, specimens of large diameter were tested to determine if there is a material sample volume effect. The results were identical to the subsize tensile data.

Degassing the material, which amounts to an anneal, reduced the yield and ultimate stresses by 53% with a slight improvement of 1.6% in

TABLE III Mechanical properties of longitudinal orientation specimens from extruded tube material

Condition	Modulus (GPa)	0.2 offset yield stress (MPa)	Ultimate tensile stress (MPa)	Elongation in 4D (%)	HRB
As-received	108.4	335.4	489.7	3.4	64.5
	108.6*	332.0*	463.0*	3.4*	
T6	103.1	375.4	517.8	3.0	85.0
Degassed	105.8	175.1	365.4	5.0	55.7
Degassed + T6	107.9	374.4	520.6	2.7	88.6
Al 6061-T6 <sup>†</sup>	69.0	275.8	310.3	17.0	91.0

\*12.8 mm diameter specimen; all other 4.1 mm diameter.

<sup>†</sup>Data from [19].

ductility (i.e. per cent elongation). Reheat-treating the degassed material to a T6 condition (degassed + T6), as shown in Table III, restores the yield and ultimate stresses exactly to the T6 level. This indicates that the concentration of magnesium was not significantly decreased in the degassing heat treatment. Vacuum degassing at higher temperatures or larger times could result in the loss of magnesium and subsequent loss of strength from precipitation hardening.

It should be noted that the T6 and the degassed + T6 thermal treatments in Table II are the standard thermal treatments for wrought Al 6061 alloys. The effect of the presence of the SiC whiskers on the solution pretreatment and ageing processes has not been extensively studied to date. Harrigan *et al.* [20] have presented results for a 30 vol % SiC particulate (SiC<sub>p</sub>)/Al 6061 alloy which indicated that solution treatments similar to those used for wrought Al 6061 are satisfactory while ageing response is accelerated in the composite SiC<sub>p</sub>/Al 6061 alloy. Similar behaviour is described by Papazian [21] for whisker material. One could then speculate that in the present treatments a slight degree of overageing might have occurred and the yield and ultimate stresses and hardness might be higher for a slightly reduced ageing time process.

### 3.2. Fractography

Observations of fracture surfaces in the SEM revealed five distinct morphological features. These features which varied widely in frequency of occurrence on the fracture surface and in decreasing frequency of observation, are:

1. Dimples — most of the fracture surface consisted of fine and equiaxed dimples of uniform size. Embedded in the base at approximately 50% of the dimples is a SiC particle tip

which according to Arsenault [22] is covered with a coating of aluminium matrix.

- Quantitative measurements of the mean dimple diameter and height measured from stereo pairs shows that the mean dimple diameter is 1.78  $\mu\text{m}$  and the mean dimple height is 0.95  $\mu\text{m}$ . Thus the dimple is slightly elongated in the tensile axis direction.

2. Inclusions — both iron-rich and chromium-rich inclusions were observed.

3. Nonbonded regions — regions of nonbonded matrix material were observed in the extruded tube material. Fig. 3a shows an example where it appears that SiC was pressed into the matrix material, but consolidation apparently did not occur during fabrication. These nonbonded regions appeared either coplanar with the plane of fracture or in the base of the so-called "fisheyes" (Fig. 3b).

4. Regions of non-infiltration — areas which lacked matrix material were rather rare. In older material, these features were more numerous, but improvements in mixing and consolidation processing have greatly reduced the frequency of these defects.

5. Decohesion at aluminium grain boundaries — occasional observation of decohesion at aluminium grain boundaries was observed. The resulting morphology is shown in Fig. 4a. The triple point void shown in Fig. 4a is not always present, but the morphology is distinguished from normal dimples by the location of the SiC at the edge of the dimple. The relative location of the boundaries and the SiC particles can be compared with the transmission electron micrograph of Fig. 4b.

### 3.3. Toughness behaviour

The effect of thermal treatment on the toughness behaviour of SiC<sub>w</sub>/Al 6061 composite material

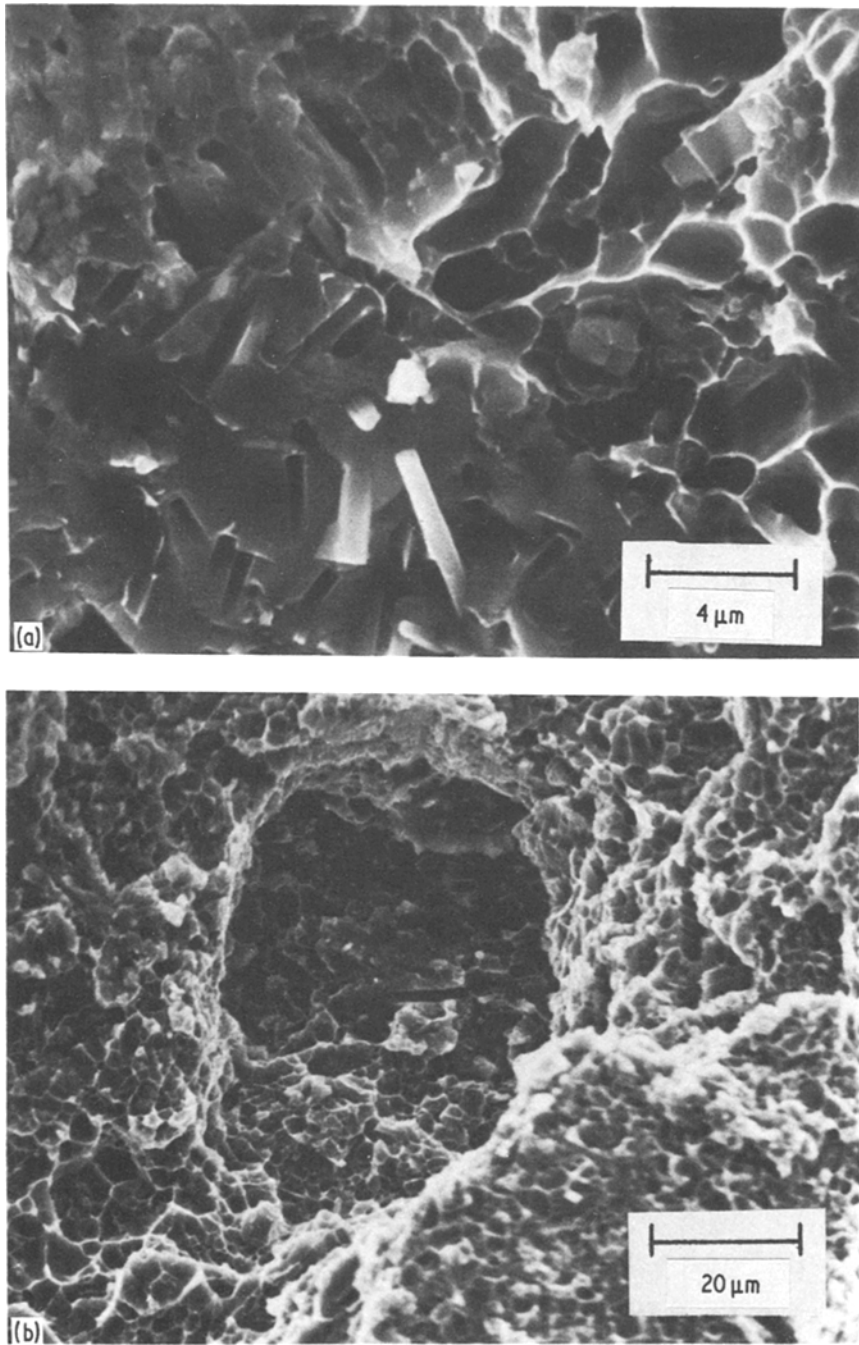


Figure 3 Example of nonbonded region in base of “fisheye” on fracture surface.

is given in Table IV. Specimen orientation was L–C. The CVN energy values are nearly the same for all the thermal treatments studied. The values are at least an order of magnitude lower than the wrought Al 6061 alloy in the T6 condition. Degassing the composite material did give the highest absorbed energy value of 1.6 J

compared to 0.5 J for the other thermal treatments. Also from macrofractographic examination about 10% shear was observed on the degassed specimens compared to zero for the others. The instrumented Charpy traces, shown in Fig. 5, further illustrate the impact energy value differences. The load–time trace for the

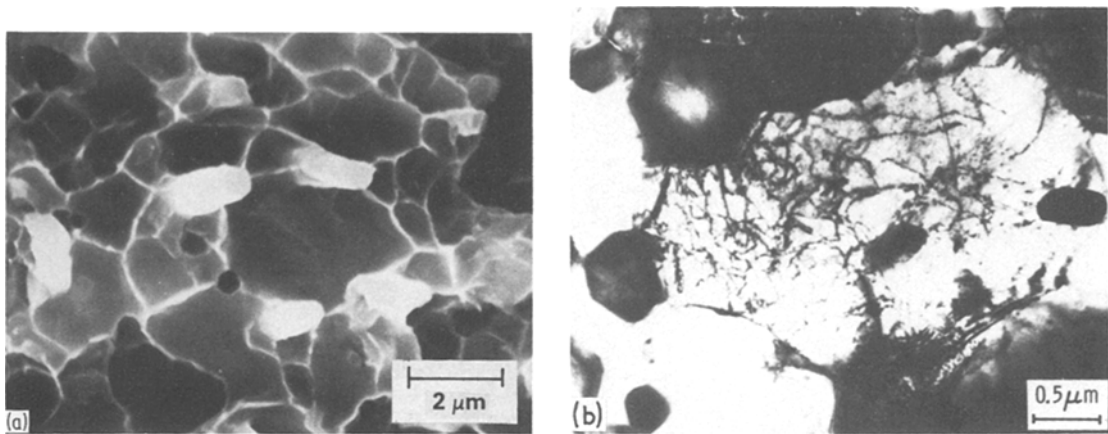


Figure 4 Fracture morphology caused by decohesion at aluminium grain boundaries. (a) SEM morphology, (b) transmission electron micrograph showing relationship of SiC whiskers to aluminium grain boundaries.

degassed material, Fig. 5a, exhibits general yielding, while the degassed + T6 shows a classic brittle behaviour. A derived dynamic stress intensity value,  $K_{Id}$ , from this test was  $19.1 \text{ MPa m}^{1/2}$ . Similar results are reported by Strife and Prewo [23].

The  $K_{Ic}$  fracture toughness values in Table IV show similar results to the Charpy energy values for the various thermal treatments. A valid  $K_{Ic}$  value for the degassed material, however, could not be determined because the ratio of  $P_{max}$  to  $P_Q$  significantly exceeded 1.10. This behaviour requires an elastic-plastic  $J_{Ic}$  test to determine the crack initiation energy. The value of  $18.9 \text{ MPa m}^{1/2}$  for the degassed material in Table IV was calculated using  $P_{max}$  and thus is conservative. The level of all  $K_{Ic}$  values for the composite are about 50% of the  $K_{Ic}$  value of  $36.8 \text{ MPa m}^{1/2}$  of wrought Al 6061 alloy in the T6 condition. This value was calculated from the  $G_{Ic}$

value of Kambour and Miller [24]. It is noted that Kambour and Miller's  $K_{Ic}$  value for Al 6061-T6 is in the range of values reported by Kaufman of 30.8 to  $50.47 \text{ MPa m}^{1/2}$  [25]. The addition of the SiC whiskers, therefore, is not completely deleterious to the fracture toughness of the Al 6061 alloy as might be expected from the high volume fraction of the silicon carbide.

The effect of orientation on the  $K_{Ic}$  fracture toughness on degassed + T6 composite material is given in Table V. The orientation of highest toughness is L-C, as also found by Crowe and Gray [13]. It is speculated that the L-C

TABLE IV Effect of thermal treatment on the toughness behaviour of SiC<sub>w</sub>/Al 6061 composite material (specimen orientation L-C)

Thermal treatment	CVN energy (J)	Fracture toughness, $K_{Ic}$ ( $\text{MPa m}^{1/2}$ )
As-received	0.5	19.5
T6	0.6	23.4
Degassed	1.6	18.9*
Degassed + T6	0.6	22.4
Al 6061-T6	23.1 <sup>†</sup>	36.8 <sup>‡</sup>

\*  $K_Q$  value based on maximum load.

<sup>†</sup> Tested by DFH on Standard CVN tester.

<sup>‡</sup> Calculated from  $G_{Ic}$  value of [24].

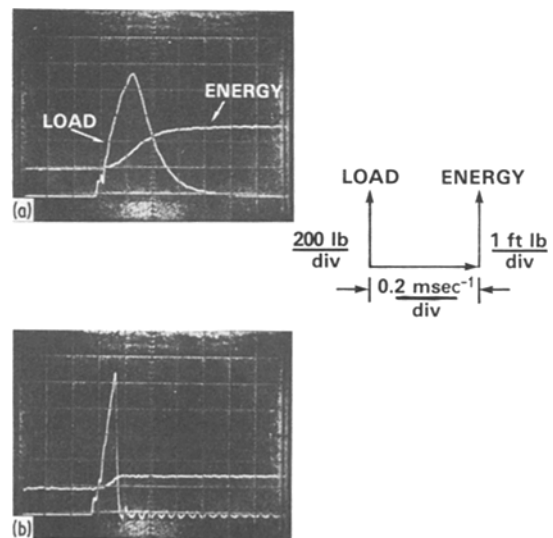


Figure 5 Instrumented Charpy V-notch load and energy against time outputs for L-C orientation SiC<sub>w</sub>/Al 6061 extruded tube materials at  $0.13 \text{ m sec}^{-1}$ . (a) Degassed, (b) degassed + T6.

TABLE V Effect of orientation on the  $K_{Ic}$  fracture toughness behaviour of degassed + T6 specimens from extruded tube

Orientation	Fracture toughness, $K_{Ic}$ (MPa m <sup>1/2</sup> )
L-C	22.4
R-L	14.0
C-L	17.6

orientation is toughest, because it has the least amount of projected area of SiC whiskers in the crack plane (i.e. the mean free path between reinforcements is the greatest).

Furthermore, SEM fractography indicates that fracture occurs by a ductile mechanism with plastic deformation localized adjacent to the crack tip. This produces a fracture surface consisting of fine dimples, as mentioned previously. The size of the dimples (2  $\mu$ m) is of the order of the size of several microstructural features such as the subgrain size of the aluminium matrix, the mean particle diameter, and the mean particle spacing. Stereo pair SEM reveals that the dimples are nearly spherical, but slightly elongated parallel to the load axis. These observations suggest that a critical strain criterion at the crack tip may control fracture. The small-scale yielding observed also suggests that fracture toughness is linked to the microstructure.

McMeeking [26] has shown from continuum mechanics that in small-scale yielding fracture, the crack tip opening displacement,  $\delta_t$ , is related to the stress intensity by the relation

$$\delta_t = \frac{\alpha K_I}{\sigma_y E} \quad (2)$$

where  $\alpha$  is a numerical constant between 0.25 and 1.0. If the fracture mechanism is associated with the nucleation, growth, and coalescence of voids, then the critical crack tip opening displacement,  $\delta_{Ic}$ , is just twice the mean dimple height and the plane strain fracture toughness,  $K_{Ic}$ , is therefore given by

$$K_{Ic} = \left( \frac{2\sigma_y E h}{\alpha} \right)^{1/2} \quad (3)$$

Using tensile data from Table III for the as-received specimen, Equation 3 predicts that  $K_{Ic}$  should range between 8.3 and 16.6 MPa m<sup>1/2</sup>, in good agreement with the present results.

#### 4. Conclusions

The following observations were made:

1. Significant increases, compared to wrought Al 6061 alloy, in modulus, yield stress, and ultimate tensile stress were observed in as-received and T6 heat treated composite materials which were obtained from an extruded SiC<sub>w</sub>/Al 6061 tube. Ductility, however, was decreased. The strength properties of the as-received tube material indicated that a T6 condition was not obtained. This was attributed to lower cooling rates following ageing in the large extrusion.

2. CVN energy values of the composite material were reduced by an order of magnitude compared to the wrought Al 6061 alloy. Thermal treatment has essentially no effect, but for the degassed thermal treatment a general yield behaviour was observed in the instrumented Charpy load-time traces.

3.  $K_{Ic}$  fracture toughness of the as-received, T6 and degassed + T6 thermal treatments was 50% of the wrought Al 6061 alloy.

4. The effect of orientation showed that the orientation with the least amount of SiC whiskers in the crack plane (i.e. greatest mean free path between reinforcements) yields the highest toughness value.

#### Acknowledgements

The authors express their appreciation for assistance to Messrs W. Willard and R. Gray in the fracture testing, Ensign M. Rennie in the instrumented Charpy V-notch testing and W. Umlandt and F. W. Rider for laboratory support. The authors also wish to acknowledge Mr J. Tydings for supplying the tube material and Mr Marlin Kinna, NAVSEA 062R, for financial assistance. Most of this work was performed while one of the authors (C.R.C.) was employed at the Naval Surface Weapons Center.

#### References

1. A. P. DIVECHA, C. R. CROWE and S. G. FISHMAN, "Failure Modes in Composites IV", edited by J. A. Cornie and F. W. Crossman (AIME, Warrendale, Pennsylvania, 1978) p. 406.
2. A. P. DIVECHA, S. G. FISHMAN and S. G. KARMARKAR, *J. Metals* **33** (1981) 12.
3. D. A. WEBSTER, in "Advances in Composite Materials", Proceedings International Conference on Composite Materials, Paris, France, edited by A. R. Bunsell, Vol. 2 (Pergamon Press, New York, 1983) p. 1165.
4. R. J. LEDERICH and S. M. L. SASTRY, *Mater. Sci. Eng.* **55** (1982) 143.
5. T. G. NIEH, *Met. Trans.* **15A** (1982) 139.

6. R. J. ARSENAULT, *Mater. Sci. Eng.* **64** (1984) 171.
7. C. R. CROWE and D. F. HASSON, in "Strength of Metals and Alloys", Vol. 2, 6th International Conference, Melbourne, Australia, edited by R. C. Gifkins (Pergamon Press, New York) pp. 859-65.
8. J. R. BOORUJY, D. F. HASSON and C. R. CROWE, US Naval Academy, Annapolis, EW-20-83, DTIC ADA134108 (1983).
9. D. F. HASSON, C. R. CROWE, J. S. AHEARN and D. C. COOKE, in "Failure Mechanisms in High Performance Materials", edited by J. G. Early and R. Shives (Cambridge University Press, New York, 1985) p. 147.
10. P. D. LAGRECA and M. MISRA, Contract Report N60921-M-4538, Martin Marietta Aerospace, Denver, Colorado, April (1983).
11. H. M. DEJARNETTE, A. P. DIVECHA and W. A. WILLARD, Naval Surface Weapons Center, Silver Spring, Maryland, NSWC TR 84-20, January (1984).
12. J. F. DOLOWY, W. C. HARRIGAN and B. A. WEBB, Phase II Final Report, Contract Report N00824-80-C-5637, Naval Sea Systems Command, Washington, DC, March (1983).
13. C. R. CROWE and R. J. GRAY, in "Failure Mechanisms in High Performance Materials", edited by J. G. Early and R. Shives (Cambridge University Press, New York, 1985) p. 157.
14. W. C. HARRIGAN, in Proceedings Sixth Annual Discontinuous Reinforced Aluminum Composite Working Group Meeting, Metal Matrix Composites Information Analysis Center, Rep. MMCIA No. 000479, Santa Barbara, California, April (1984) p. 211.
15. J. M. COX and D. CHELLAN, *ibid.* p. 167.
16. R. J. GOODE, *Materials Research and Standards, MISRA, Amer. Soc. Testing Mater.* **12** (9) (1972).
17. ASTM E. 399-78, "1978 Annual Book of ASTM Standards", Part 10 (ASTM Philadelphia, Pennsylvania, 1978).
18. C. R. CROWE, R. A. GRAY and D. F. HASSON, NRL Memo Rpt 5417 (Naval Research Laboratory, Washington, DC, 1985).
19. "Metals Handbook", 8th Edn., Vol. 1, "Properties and Selection of Materials", edited by T. Lyman (American Society for Metals, Metals Park, Ohio, 1961), p. 964.
20. W. C. HARRIGAN, M. T. RISTOW, J. F. DOLOWY and B. A. WEBB, presented at TMS-AIME 112th Annual Meeting Atlanta, Georgia, 6-10 March 1983 (AIME, Warrendale, Pennsylvania).
21. J. M. PAPAIZIAN, in Proceedings Sixth Annual Discontinuous Reinforced Aluminum Composite Working Group Meeting, MMCIA Report No. 00479, Santa Barbara, California, April 1984 (AIME, Warrendale, Pennsylvania) p. 223.
22. R. J. ARSENAULT, *ibid.*, p. 1.
23. J. R. STRIFE and K. M. PREWO, United Technologies Research Center, Report No. R82-916176-1, December (1982).
24. R. P. KAMBOUR and S. MILLER, *J. Mater. Sci.* **12** (1977) 2281.
25. J. G. KAUFMAN, in "Fracture Prevention and Control", edited by D. W. Hoepfner (American Society for Metals, Metals Park, Ohio, 1974) pp. 121-41.
26. R. M. McMEEKING, *J. Mech. Phys. Solids* **25** (1977) 357.

*Received 10 December 1984  
and accepted 15 January 1985*